Genetics in Medicine (2026) 28, 102531

ELSEVIER

Genetics in Medicine
An Official Journal of the ACMG

www.journals.elsevier.com/genetics-in-medicine

ARTICLE

Biallelic *LAMP3* variants in 5 families with interstitial lung disease: Evidence of a disease-gene association

Laura A. Keehan[1], Hitomi Ono-Minagi[2,3], Mohamad Hadhud[4], Jonathan Rips[5], Daniel M. Hinds[6], Anthony J. Fischer[6], Jennifer A. Bartlett[6], Paul B. McCray[6], Nada Qawasmi[4,7], Nadia Nathan[8,9], Camille Louvrier[8], Tifenn Desroziers[8], Markus Damme[10], Matthias Griese[11], Daniel J. Wegner[12], F. Sessions Cole[12], Jennifer A. Wambach[12], Matthew T. Wheeler[13,14], Peter D. Burbelo[2], Devon E. Bonner[1,13], Undiagnosed Diseases Network[13], Jonathan A. Bernstein[1,13], John A. Chiorini[2], Oded Breuer[4], Carlos Milla[15,*]

ARTICLE INFO

Article history:
Received 1 May 2025
Received in revised form
20 January 2026
Accepted 27 January 2026
Available online 3 February 2026

Keywords:
Interstitial lung disease
LAMP3
Surfactant dysfunction

ABSTRACT

Purpose: Genetic causes of surfactant dysfunction are associated with childhood interstitial lung disease. Lysosome-associated membrane glycoprotein 3 (*LAMP3*) is highly expressed within lamellar bodies of alveolar epithelial type II cells, and variants in *LAMP3* have recently been suggested as a novel cause of childhood interstitial lung disease. This study describes the phenotypes of participants with biallelic variants in *LAMP3* and presents functional studies evaluating the role of specific *LAMP3* variants.

Methods: Phenotypic data were collected through chart review and clinical evaluation. In vitro effects of *LAMP3* variants were evaluated through immunohistochemistry, western blot, and flow cytometry.

Results: Thirteen participants were identified with biallelic variants in *LAMP3*. They presented with variable phenotypes ranging from neonatal respiratory distress to asymptomatic in adulthood. All symptomatic participants demonstrated ground glass opacities early in life and lung fibrosis later in life. For 1 participant, BAL analysis showed abnormal surfactant protein composition and lung biopsy revealed irregular lamellar bodies. In vitro studies in lung epithelial cells with induced expression of specific *LAMP3* variants demonstrated reduced protein expression and abnormal glycosylation.

Conclusion: Biallelic *LAMP3* variants are associated with an interstitial lung disease phenotype with variable expressivity. Evaluation for *LAMP3* variants should be considered in individuals with unexplained interstitial lung disease.

Laura A. Keehan, Hitomi Ono-Minagi, and Mohamad Hadhud contributed equally to this work and designated as co-first authors.
John A. Chiorini, Oded Breuer, and Carlos Milla are co-senior authors.
The names of the Undiagnosed Diseases Network members will appear at the end of the article.

*Correspondence and requests for materials should be addressed to Carlos Milla, Department of Pediatrics, Division of Pulmonary Medicine, Stanford University School of Medicine, Pediatric Pulmonology, 770 Welch Road, Suite 350, Stanford, CA 94304. *Email address:* cmilla@stanford.edu
Affiliations are at the end of the document.

doi: https://doi.org/10.1016/j.gim.2026.102531

Introduction

Surfactant is produced by alveolar epithelial type II (AT2) cells and stored in lamellar bodies (LB) before being secreted into the alveolar space via exocytosis.[1] Surfactant metabolism is regulated by proteins involved in lipid trafficking, transcriptional regulation, transport, and degradation.[2,3] Defects in surfactant production and function are associated with neonatal respiratory failure and interstitial lung disease (ILD).[4] To date, genes associated with disruption of surfactant metabolism include: ATP-binding cassette transporter A3 (*ABCA3,* MIM #610921), surfactant protein B (*SFTPB,* MIM #265120), surfactant protein C (*SFTPC,* MIM #610913), NK2 homeobox 1 (*NKX2-1,* MIM #610978), surfactant protein A1 (*SFTPA1*, MIM #178360), and surfactant protein A2 (*SFTPA2*, MIM #178642).[1,5,6] The age of onset and severity of disease varies depending on the genotype.[5,7,8] For example, infants with biallelic loss-of-function variants in *SFTPB* and *ABCA3* present with severe neonatal respiratory failure; however, there can be variable clinical outcomes in infants, children, and adults with partial function *ABCA3* variants.[9-12] In addition, pulmonary phenotypes associated with *SFTPC* and *NKX2-1* variants include severe neonatal respiratory failure, ILD, adult pulmonary fibrosis, and lung cancer.[13-17]

Lysosome-associated membrane glycoprotein 3 (*LAMP3*) is a transmembrane protein highly expressed in lung tissue and dendritic cells.[18] In the lung, LAMP3 localizes specifically to LBs within AT2 cells.[19,20] Overexpression studies have shown that LAMP3 alters trafficking of membrane proteins and induces lysosomal disruption.[21] LAMP3 is thought to be involved in the trafficking and regulation of surfactant components.[19,22-24] Studies using LAMP3-deficient mice indicate that a lack of LAMP3 disrupts the balance of surfactant proteins, leading to altered surfactant functionality and increased airway resistance under induced asthma conditions.[22] Additionally, a study on fatal neonatal respiratory distress in dogs identified a homozygous missense variant in *LAMP3* p.(Glu387Lys) that results in defective lamellar body formation.[25] In humans, a recent semi-automated genotype-phenotype matching study identified *LAMP3* as a candidate disease gene for ILD.[26] This was further confirmed by the report of the functional consequences of biallelic *LAMP3* variants in a child with fibrosing ILD.[27]

Here, we report 13 participants from 5 unrelated families with biallelic missense or frameshift variants in *LAMP3*. These participants presented with variable pulmonary phenotypes ranging from clinically asymptomatic to severe neonatal respiratory failure and ILD. Additionally, we use a human lung epithelial cell line (A549) transiently transfected with 2 of the identified missense variants in *LAMP3* to show decreased LAMP3 protein expression, endoplasmic reticulum (ER) stress and induction of cell death through activating apoptotic pathways. The *LAMP3* variants identified in these participants offer a plausible explanation for their pulmonary disease and provide evidence of a disease-gene association for biallelic *LAMP3* variants in humans.

Materials and Methods

Human participants and genetic analysis

Legally authorized representatives provided informed consent for all participants. Participants were identified through GeneMatcher, the pediatric European ILD registry, the Undiagnosed Diseases Network,[28] and professional communication. Participant 1 was enrolled in the Undiagnosed Diseases Network (NHGRI protocol 15HG0130). Participants 2a-2c were enrolled in a research study focused on rare genetic diseases at Washington University in St Louis. Participants 3a-3g were enrolled in a research study evaluating unbiased semi-automated genotype-phenotype matching algorithm.[26] Participant 4a was enrolled from an exome database at the Hadassah Hebrew University. Participant 5 was enrolled in the childhood ILD genetic project approved by the ethical authorities (Comité de protection des personnes n°20130604).[27]

For each family, the probands (participants 1, 2a, 2b, 3a, 3e, 4, and 5) underwent either exome or genome sequencing. No pathogenic or likely pathogenic variants were identified in genes associated with surfactant deficiency or ILD, including *ABCA3*, *SFTPB*, *SFTPC*, *NKX2-1*, *SFTPA1*, and *SFTPA2*. *LAMP3* variants were confirmed for segregation analysis by Sanger sequencing. Variants are reported in the GRCh37 genome build. Phenotypic and genetic information was collected from medical record review and clinical evaluation.

Lung biopsy, bronchoalveolar lavage processing, and western blot (WB) analysis

Lung tissue was fixed in 10% formalin and paraffin-embedded sections were prepared according to standard methods and stained with hematoxylin and eosin, Schiff's periodic acid, and Masson's trichrome for light microscopy. A fresh section was fixed in 2% glutaraldehyde and 4% paraformaldehyde in 100 mM Na cacodylate buffer and processed for electron microscopy (EM). The pooled supernatant from BAL fluid (3× 1 ml 0.9% NaCl/kg bw) was stored frozen at −80 °C. Total protein was determined by the method of Bradford. Surfactant protein (SP)-B, SP-C, proSP-B, and proSP-C were determined under nonreducing conditions as described previously.[29,30]

Modeling of the human LAMP3 protein

Using the full-length human LAMP3 protein, the predicted structures were obtained as provided from the AlphaFold algorithm and protein structure database (https://alphafold.ebi.ac.uk). Structure visualization was performed using

PyMOL (The PyMOL Molecular Graphics System, Version 2.0 Schrödinger, LLC).

Expression vectors for analysis of LAMP3 variant proteins

The pME18S-empty and pME18S-LAMP3 mammalian expression vectors were used for the in vitro study of LAMP3. Two *LAMP3* variants were generated using Q5 Site-Directed Mutagenesis Kit (New England Biolabs). The full nucleotide sequences of these variants were confirmed by Sanger sequencing.

Lung epithelial cell transient transfection for immunofluorescence and flow cytometry

Human lung carcinoma epithelial cells (A549) were transiently transfected with plasmids using Lipofectamine 3000. Cells were harvested for flow cytometry 48 hours after transfection. The Immunofluorescence analysis was performed as described previously.[31] Flow cytometry data were analyzed using FlowJo software, v10.10.0 (BD Biosciences).

WB analysis of LAMP3 variants

To study the effect of the *LAMP3* variants on protein stability, WB analysis was performed. Transfected cells were lysed in radioimmunoprecipitation assay buffer (Santa Cruz Biotechnology) supplemented with protease and phosphatase inhibitors. Cell lysates were analyzed using the JESS Simple Western™ instrument (Protein Simple) per the manufacturer's instructions.

Cell growth and apoptosis analysis of LAMP3 variants

After trypsinization of transfected A549 cells, apoptotic cells were detected using the transferase dUTP nick end labeling (TUNEL) assay Kit and flow cytometry with 7-AAD (ab66110, Abcam) and the BD FACSymphony (BD Biosciences). The cell growth analysis was performed as described previously.[31]

Expression of LAMP3-green fluorescent protein (GFP) and LAMP3-Ala13Glu in A549 cells

cDNA sequences for wild-type *LAMP3* and the *LAMP3*-Ala13Glu variant were cloned into the pHAGE lentiviral backbone plasmid upstream of the gene for *Aequorea coerulescens* GFP (AcGFP).[32] To express the GFP-tagged proteins in A549 cells, cells were grown in 12-well plates and transiently transfected with the plasmid constructs (1 µg plasmid/well) using Lipofectamine LTX reagent (Thermo Fisher Scientific). At 24 hours after transfection, cell lysates were prepared using radioimmunoprecipitation assay buffer (Sigma Aldrich) containing the Roche cOmplete Mini EDTA-free Protease Inhibitor Cocktail (Sigma Aldrich). Lysates were stored at −80 °C until use and total protein concentrations were estimated using the Pierce BCA Protein Assay Kit (Thermo Fisher).

To visualize proteins by WB, samples (20 µg total protein/lane) were resolved by SDS-PAGE on a 4% to 20% Mini-PROTEAN TGX precast gel (Bio-Rad Laboratories). Proteins were transferred to polyvinylidene difluoride membranes (Immobilon-FL, Sigma Aldrich), then blocked for 1 hour with 0.1% Hammarsten casein. The membrane was probed with anti-GFP antibody (Takara Bio catalog no. 632592; Takara Bio) and anti-beta actin (Sigma Aldrich catalog no. A2228) overnight at room temperature. The membrane was washed with TBS-Tween 4 times (5 minutes each), then incubated for 1 hour with fluorescent secondary antibodies (IRDye 800CW Donkey anti-Rabbit IgG + IRDye 680LT Donkey anti-Mouse IgG; LI-COR) at a 1:10,000 dilution. After 5 5-minute washes with TBS-Tween, fluorescent bands were visualized on an Odyssey M imager (LI-COR).

Statistics

The data are presented as the mean values with standard deviations. Paired *t* test was used to compare the means of the empty vector, and values of $P < .05$ were considered significant.

Results

Clinical case summaries

Key phenotypic and genotypic information for all participants is summarized in Supplemental Table 1. Detailed clinical descriptions of the participant phenotypes are presented in Supplemental Material 1.

Family 1

An affected female was found to have a homozygous single-nucleotide deletion in *LAMP3* NM_014398.4:c.247del p.(Ile83PhefsTer47) predicted to produce a frameshift and early stop gain of the canonical 416 amino acid protein. Both parents are heterozygous for this variant and consanguinity was denied. This variant is rare in a large adult database (gnomAD v4.1.0, minor allele frequency (MAF) 2.23e−5, accessed March 2025) with no homozygous individuals reported.[33] Clinically, she presented with severe neonatal respiratory failure. She has a lifelong history of oxygen dependence, and serial lung CT studies demonstrate a progression from ground glass opacities (GGO) in early life to fibrotic changes in adolescence (Figure 1A). Lung biopsy at age 18 months showed a nonspecific interstitial pneumonitis pattern compatible with chronic pneumonitis of infancy (Figure 1B). Transmission electron microscopy (TEM)

showed AT2 cells with irregular lamellar bodies that contained dense, round inclusions consistent with surfactant protein dysfunction (Figure 1C). Biochemical analysis of BAL supernatant for hydrophobic surfactant proteins demonstrated a small amount of proSP-B, undetectable mature SP-B, abundant mature SP-C, mainly in its monomeric form, and no aberrant proSP-C processing forms (Figure 1D). Lack of sibling availability precluded *LAMP3* variant segregation testing.

Family 2

Three siblings (2a-c) were found to be compound heterozygous for missense variants in *LAMP3* NM_014398:c.38C>A p.(Ala13Glu) and NM_014398:c.1162G>A p.(Gly388Arg). Both parents are heterozygous for one of the variants (Figure 2B). The p.(Ala13Glu) variant is extremely rare (gnomAD v4.1.0, MAF 6.47e−7) with no homozygous individuals reported and is predicted to be deleterious (CADD score 17.4).[34] The p.(Gly388Arg) variant is extremely rare (gnomAD v4.1.0, MAF 6.22e−7) with no homozygous individuals reported and predicted to be deleterious (CADD score 25.6). The p.(Gly388Arg) variant lies within the predicted single transmembrane domain (p.382-402), and the p.(Ala13Glu) variant is predicted to alter the signal peptide (AA 1-27), suggesting alterations in processing and subcellular localization. The older female siblings (2a and 2b) presented with severe neonatal respiratory failure, experienced significant respiratory morbidity and failure to thrive early in life, and had lung CT imaging that demonstrated GGO and cystic lung disease (Figure 1E). Over time, they have also developed obstructive lung disease. In contrast, their younger brother (2c), who is also compound heterozygous for the same *LAMP3* variants, has no history of respiratory symptoms and had unremarkable lung CT imaging at age 14 months.

Family 3

Seven participants (3a-g) from a consanguineous extended family (Figure 2C) were found to be homozygous for a missense variant in *LAMP3* NM_014398.4:c.862G>A p.(Gly288Arg). This residue is highly conserved and extremely rare (gnomAD v4.1.0, MAF 1.43e−5) with no homozygous individuals reported and is predicted to be deleterious (CADD score 28). This family was briefly described by Rips et al[26] (2024). Four male participants (3a, 3c, 3d, and 3e) in this family have a lifelong history of respiratory disease, and 2 of them (3a and 3e) presented with severe neonatal respiratory failure. All 4 symptomatic participants had imaging studies that demonstrated GGO with progression to fibrotic changes (Figure 1F and G). One symptomatic participant (3c) had a lung biopsy demonstrating interstitial infiltration compatible with chronic pneumonitis of infancy. The oldest symptomatic participant (3d) had advanced lung disease with extensive fibrotic

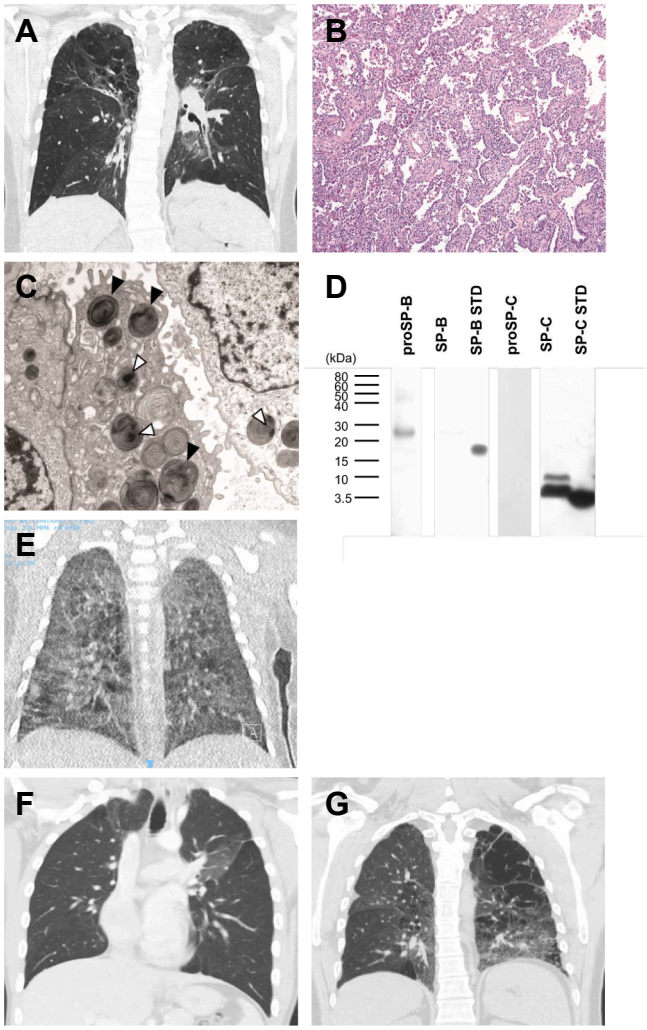

Figure 1 Macroscopic and microscopic imaging studies from participants with biallelic *LAMP3* variants. A. CT chest from participant 1 at age 13 years shows ground glass opacities (GGO), cystic changes especially of the upper lobes, and honeycombing. B. Hematoxylin and eosin staining of a lung section from participant 1. Pathology findings on lung biopsy of participant 1 demonstrate preserved parenchymal architecture with non-specific interstitial pneumonitis pattern and diffuse cellular expansion with widening of interstitial spaces. C. Transmission electron microscopy (TEM) of lung biopsy tissue from participant 1 demonstrates lamellar bodies of alveolar epithelial type II (AT2) cells with disrupted myelin organization (black arrowhead) and round dense inclusions (white arrowheads). D. WB analysis of the hydrophobic surfactant proteins and their precursors in BAL supernatant of participant 1, which demonstrates absence of surfactant protein (SP)-B in contrast to abundant SP-C (spliced compilation of individual protein blots with standards loaded at 9 ng for SP-B and 10 ng for SP-C). E. CT chest from participant 2b at age 2-months shows diffuse septal thickening, GGO, and cystic changes. F. CT chest from participant 3c at age 22 years shows GGO in the upper lobes bilaterally. G. CT chest from participant 3d at age 40 years before lung transplant shows diffuse emphysematous and fibrotic changes.

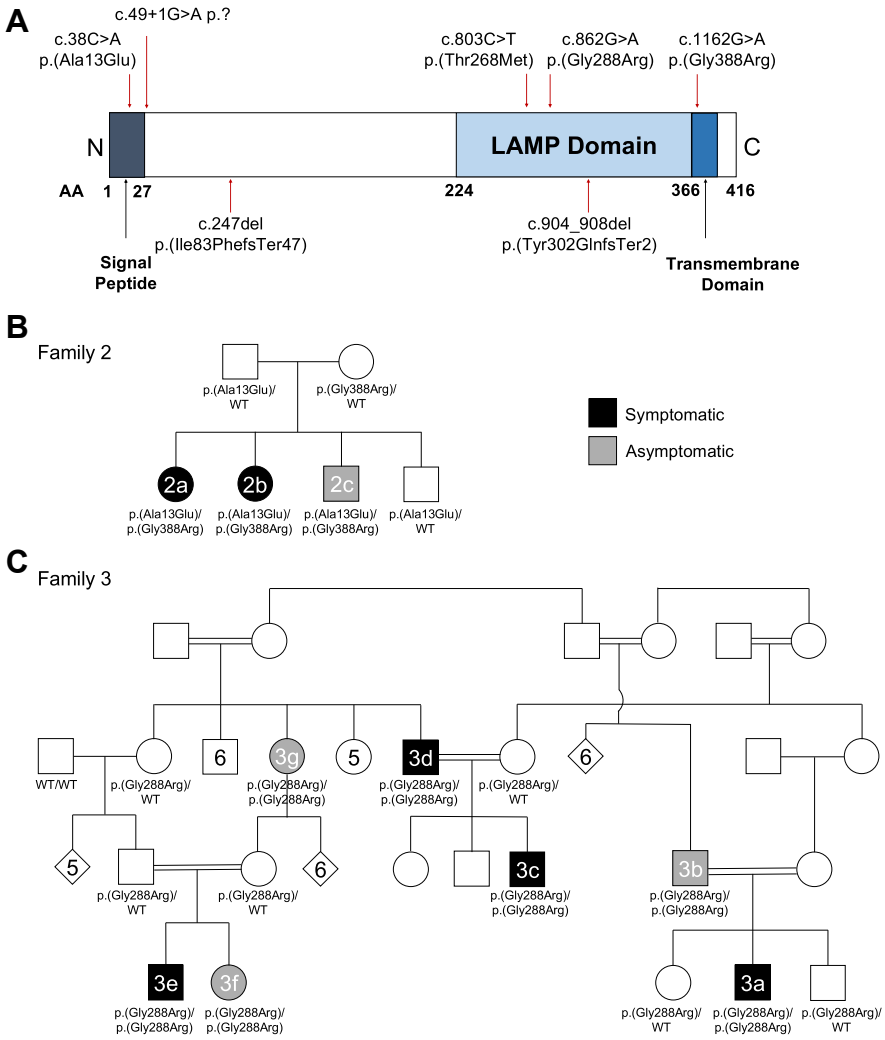

Figure 2 Pedigrees for (B) family 2 and (C) family 3. For compound heterozygous or homozygous participants, black shapes represent symptomatic participants, and gray shapes represent asymptomatic participants. Participant identifiers are included inside the designated shape for all participants described in this report. For all participants who completed genetic testing (either exome sequencing for participants 2a, 2b, 3a, and 3e or Sanger sequencing in all other participants), genotype is included below. A. Schematic of LAMP3 functional domains, including the signal peptide, LAMP domain, and transmembrane domain. Location of *LAMP3* variants identified in this cohort are indicated with arrows.

honeycombing on imaging studies and underwent lung transplantation at age 50 years. Three homozygous participants in this family are clinically asymptomatic (3b, 3f, 3g). At age 38, 1 asymptomatic male participant (3b) underwent a chest CT scan that revealed areas of GGO and uneven aeration. The remaining 2 homozygous female participants (3f and 3g) are asymptomatic at ages 4 years and 47 years, respectively. The younger asymptomatic participant (3f) had normal lung CT imaging at age 3 years, normal development, no hospital admissions, and normal respiratory physical exam. Participant 3g was unavailable for further clinical evaluation. Additional chest CT images from participants 3a, 3b, 3c, and 3e are presented in Supplemental Figures 1-4.

Family 4

A single affected male participant was found to be homozygous for an intronic variant in *LAMP3* NM_014398.4:c.49+1G>A p.?. This variant is rare (gnomAD v4.1.0, MAF: 1.16e−5) with no homozygous individuals identified in gnomAD and is predicted to disrupt a splice donor site (CADD score 33, SpliceAI 0.99).[35] This participant presented with severe neonatal respiratory failure, and lung imaging studies demonstrated diffuse GGO with uneven aeration at age 2 years.

Family 5

A single affected male was found to be compound heterozygous for missense and frameshift variants in *LAMP3* NM_014398 c.803C>T p.(Thr268Met) and c.904_908del

p.(Tyr302GlnfsTer2). This participant was described previously by Louvrier et al.[27] The p.(Thr268Met) variant is rare (gnomAD v4.1.0, MAF: 6.08e−5) with no homozygous individuals reported and predicted to be deleterious (CADD 26.2). The p.(Tyr302GlnfsTer2) variant is rare (gnomAD v4.1.0, MAF 1.31e−4) with no homozygous individuals reported and predicted to cause a frameshift and early stop gain. Functional studies of the missense variant showed reduced levels of mutant protein, impaired N-glycosylation and protein instability, and altered interactions between LAMP3 and SP-B and SP-C.[27] This participant has a complex past medical history of failure to thrive, growth hormone deficiency, and developmental delay but did not develop respiratory symptoms until 9-years-old. Lung imaging studies demonstrated GGO, and lung biopsy revealed thickened alveolar walls resembling usual interstitial pneumonitis and a slightly decreased Pro-SP-B and SP-B staining.

Case comparison

Overall, we present 13 participants with biallelic variants in *LAMP3* from 5 families who presented with variable respiratory phenotypes that range from neonatal respiratory failure and progression to significant ILD with airway obstruction to clinically asymptomatic adults. Of the symptomatic participants, 6 of 9 (66%) presented with neonatal respiratory failure requiring mechanical ventilation. The other 3 of 9 (33%) participants presented with dyspnea starting in the first year of life or later in childhood. GGO were observed on chest CT for all 9 symptomatic participants. Those who had follow-up imaging later in life showed progression to fibrotic changes. A variety of medications including oral, inhaled, and intravenous steroids, hydroxychloroquine, inhaled short- and long-acting beta-2 agonists, and leukotriene receptor antagonists were used with inconsistent clinical responses. Supplemental oxygen was needed for 4 participants, and 1 participant required lung transplantation at age 50 years. Overall, symptomatic participants presented with broad phenotypic variability without consistent response to specific medications. Four out of 13 participants (31%) with biallelic *LAMP3* variants had no overt clinical respiratory symptoms. Interestingly, participant 3b had GGO identified on chest CT at age 38 years despite having no reported clinical symptoms. Chest imaging was normal in 2 asymptomatic participants (2c and 3f) and not completed in the one other asymptomatic participant. No heterozygous participants were reported to have respiratory symptoms within these families, but they were also not specifically evaluated for subclinical manifestations of disease. Familial variant testing was unable to be completed for siblings within families 1, 4, and 5.

Within this cohort of participants, there is no discernible correlation of clinical severity to sex or genotype. These variants occur throughout the *LAMP3* transcript. However, the missense variants appear to cluster within the signal peptide, transmembrane, and LAMP3 domains (Figure 2A). We classified the variants according to the American College of Medical Genetics and Genomics (ACMG) and the Association for Molecular Pathology criteria.[36] PVS1 was applied to null variants predicted to result in nonsense-mediated decay. PS3 was applied when functional assays performed in this study or in Louvrier et al[27] provided evidence supporting pathogenicity. PM2_Supporting was applied to variants that are rare (highest MAF < 0.1%) and with no homozygous occurrences in gnomAD v4.1. PM1_Supporting was applied to variants located within protein functional regions; specifically, the signal peptide (amino acids 1-27), the LAMP domain (amino acids 124-382) and the transmembrane domain (amino acids 382-402). Based on these criteria, the variants were classified as likely pathogenic as outlined in Supplemental Table 2. In addition, we evaluated the clinical validity of the gene-disease association according to the Clinical Genome Resource (ClinGen) framework.[37] Based on these criteria, the strength of this gene-disease association was strong as outlined in Supplemental Table 3.

Structural modeling of the LAMP3 p.(Gly288Arg) and p.(Gly388Arg) variants

Protein sequence alignment of LAMP3 across species revealed that the p.(Gly288Arg) substitution identified in family 3 involves a highly conserved position with no variations observed in any species except for a semi-conservative change (Gly to Ser) found in Xenopus (Supplemental Figure 5A). Similarly, the p.(Gly388Arg) substitution seen in family 2 also involves a highly conserved amino acid residue seen in LAMP3 proteins from other species (Supplemental Figure 5B). Additional analysis comparing these amino acid positions with the 4 other human LAMP family members revealed that these amino acid positions are highly conserved (Supplemental Figure 5C and D).

Three-dimensional modeling using PyMOL (Schrödinger, LLC [2015] The PyMOL Molecular Graphics System, Version 2.3.0.) demonstrated that the amino acid substitutions resulting from these p.(Gly288Arg) and p.(Gly388Arg) variants likely alter protein structure (Supplemental Figure 5E-I). The p.(Gly288Arg) is located in a β-strand rich region in a β-turn, likely interfering with proper formation of the β-sheet. The p.(Gly388Arg) variant is located within a transmembrane region, which is largely hydrophobic. The replacement of glycine with the charged arginine residue causes a predicted stability change (ΔΔG) using MCM-membrane yielded a value of −0.645 Kcal/mol, indicating that this amino acid substitution is destabilizing (Supplemental Figure 5I and data not shown). Based on these findings, these 2 LAMP3 variants may have impaired stability with lamellar body membrane integration.

Induced expression of *LAMP3*-Gly288Arg and *LAMP3*-Gly388Arg variants reduces lung epithelial cell proliferation

The *LAMP3*-Gly288Arg and *LAMP3*-Gly388Arg variants underwent in vitro functional characterization. Confocal

imaging of transiently transfected *LAMP3* wild type (WT) and variant constructs into A549 pulmonary epithelial cell line revealed protein staining on the lysosomal membrane (Supplemental Figure 5J). WB of whole cell lysate from transiently transfected cells suggested that the *LAMP3*-Gly288Arg and *LAMP3*-Gly388Arg variants showed decreased expression compared with *LAMP3*-WT (Figure 3A and B). Cell proliferation was reduced in *LAMP3*-Gly288Arg and LAMP3-Gly388Arg, with this reduction being more prominent in LAMP3-Gly388Arg cells (Figure 3C and D). These results suggest that, compared with the WT protein, the *LAMP3*-Gly288Arg and *LAMP3*-Gly388Arg amino acid substitutions inhibit cell proliferation in a human pulmonary epithelial cell line.

LAMP3-Gly388Arg variant induces lung epithelial cell apoptosis

To determine whether the changes observed in cell proliferation with the LAMP3 variants were the result of alterations in cell cycle or increased apoptosis, the cell cycle was analyzed in cells transfected with plasmids expressing control empty vector, *LAMP3*-WT, and *LAMP3* variants by TUNEL, 7-AAD cell viability staining, and flow cytometry. Bright-field microscopy showed significant blebbing in both the *LAMP3*-Gly288Arg and *LAMP3*-Gly388Arg transfected cells (Figure 3E-H). Cells expressing *LAMP3*-Gly288Arg and *LAMP3*-Gly388Arg exhibited similar profiles by flow cytometry (Figure 3I-L). However, cells expressing *LAMP3*-Gly388Arg had a significantly higher proportion of TUNEL-positive cells compared with cells that express *LAMP3*-Gly288Arg or *LAMP3*-WT (Figure 3M-P). Moreover, the percentage of TUNEL-positive/7-AAD-positive cells was also significantly elevated (Figure 3P), suggesting that these cells were either in the late stages of apoptosis or undergoing cell death due to necrosis. These findings suggest that the cell death was increased in the cells expressing *LAMP3*-Gly388Arg compared with the *LAMP3*-WT.

Changes in both plasma and mitochondrial membrane protein expression are reported to trigger apoptosis.[38] Because these mechanisms can be broadly divided into intrinsic and extrinsic pathways, the localization of Galectin-3 (Gal3) was examined to distinguish between the 2 apoptotic pathways.[39] An increase in the number of cells with Galectin-3 puncta in the cytoplasm compared with WT suggests that the intrinsic apoptotic pathway is likely involved (Figure 4A-C).

Caspase-3 and Caspase-8 are critical regulators of the apoptotic response, with Caspase-8 being particularly important for initiating apoptosis. Although the activation of cleaved Caspase-8 (cCas8) was not detected in WB analysis of protein from cells that express *LAMP3*-Gly288Arg or *LAMP3*-Gly388Arg, a significant increase in cleaved Caspase-3 (cCas3) was observed. This finding, combined with the activation of Cas3 and the inactivation of Cas8, suggests that apoptosis is increasing (Figure 4D-G).

Lastly, ER stress signals were assessed in A549 cells transfected to express these *LAMP3* variants, given that increased ER stress could potentially enhance Caspase-3 activity and promote apoptosis.[40] Cells that expressed both the *LAMP3*-Gly288Arg or *LAMP3*-Gly388Arg variants showed a significant increase in Bip and protein disulfide isomerase proteins—particularly in cells expressing the *LAMP3*-Gly388Arg variant (Figure 4H-K). Taken together, these results suggest that the *LAMP3* variants enhance ER stress and the caspase pathway, leading to the induction of apoptosis (Figure 4L).

The *LAMP3*-Ala13Glu variant exhibits dramatically reduced protein abundance

In silico prediction using the SignalP server indicates a high probability that the LAMP3 protein harbors an N-terminal signal peptide for sorting into the secretory pathway and that the alanine to glutamic acid change at residue 13 seen in the *LAMP3*-Ala13Glu variant disrupts this signal peptide (Figure 5A).[41] To explore the effects of this variant on LAMP3 expression and protein processing, we used transient transfection to express GFP-tagged versions of this variant and the wild-type protein in A549 cells and visualized the proteins in cell lysates by WB (Figure 5B). There was substantially lower overall expression of the *LAMP3*-Ala13Glu variant relative to the wild-type protein, as well as notable differences in the apparent molecular weight and processing of the protein. For wild-type LAMP3, we observed 2 prominent bands: one at approximately 80 kDa, consistent with the predicted molecular weight for fully glycosylated GFP-tagged LAMP3 and a second band at ~160 kDa, possibly indicating dimer formation. An additional lower molecular weight band could also be detected at around 70 kDa, which is the expected size of unglycosylated GFP-tagged LAMP3. For the *LAMP3*-Ala13Glu variant, only this lowest molecular weight band was seen, indicating that this variant is likely not glycosylated. These results suggest that disruption of the signal peptide in the *LAMP3*-Ala13Glu variant has a detrimental effect on maturation, trafficking, and glycosylation of the protein due to loss of targeting to the secretory pathway.

Discussion

This study identifies biallelic variants in *LAMP3* as a genetic cause of human ILD presenting with a broad spectrum of pulmonary symptoms. Functional studies in lung epithelial cells demonstrate that some of the *LAMP3* variants identified in this cohort cause decreased cell proliferation, induced ER stress, activation of apoptotic pathways, or abnormal protein glycosylation. Lung biopsy and BAL analysis from participant 1 demonstrated abnormal LBs and altered surfactant protein composition. Altogether, these

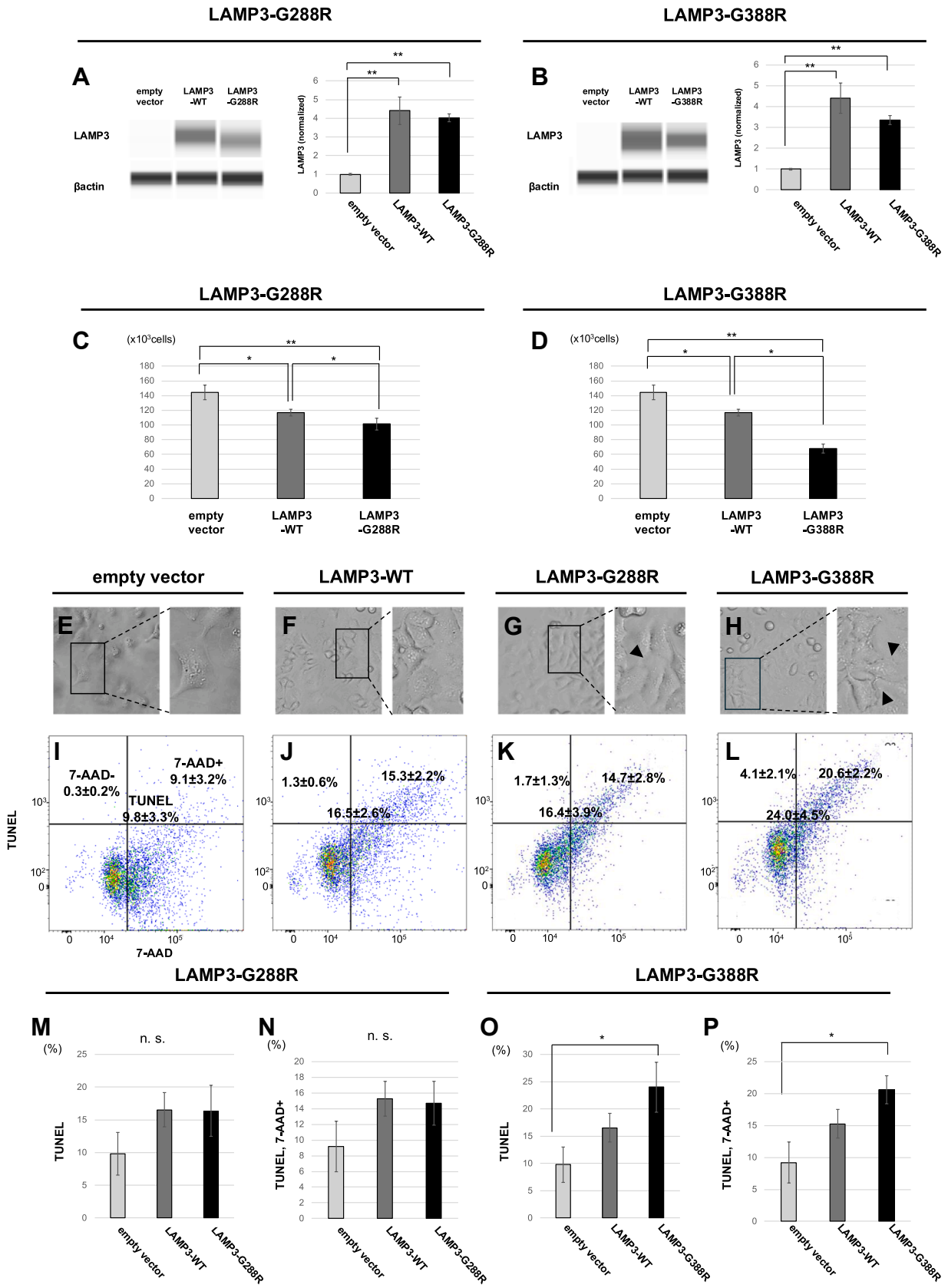

Figure 3 ***LAMP3*** **variants effect on A549 epithelial cell proliferation.** A and B. *LAMP3* variant expression. A549 cells were treated with pME18S-empty plasmid (as negative control), pME18S-*LAMP3*-WT plasmid (as positive control), or pME18S-*LAMP3*-Gly288Arg (LAMP3-Gly288Arg) (A), or pME18S-*LAMP3*-Gly388Arg (*LAMP3*-Gly388Arg) (B) and WB was performed 24 hours after transfection. Differences in the expression of LAMP3/β-actin in WB compared with transfected cells with empty vector, *LAMP3*-WT, or *LAMP3*-

findings provide further evidence of a disease-gene association for *LAMP3* in humans and highlight the need for further research to clarify role of *LAMP3* in surfactant metabolism and ILD pathogenesis.

LAMP3 is constitutively expressed in AT2 cells and transiently expressed in the major histocompatibility complex class II compartment of dendritic cells (DCs).[19,42,43] Functional and structural similarities between DCs and AT2 cells suggest a possible role of LAMP3 in the exocytosis of LBs in AT2 cells.[44,45] Additionally, LAMP3-positive vesicles are involved in the maturation and processing of surfactant components, suggesting a role for LAMP3 in surfactant homeostasis.[43] Given its function in AT2 cells and surfactant biology, LAMP3 dysfunction is plausibly linked to the development of ILD.

Animal models have demonstrated a link between LAMP3 dysfunction and pulmonary phenotypes. Dillard et al[25] identified a cohort of terrier dogs with lethal neonatal respiratory failure, and exome sequencing revealed that all affected dogs were homozygous for a *LAMP3* missense variant XM_843796.4:c.1159G>A p.(Glu387Lys). This variant is predicted to disrupt a structurally important disulfide bond. The affected animals had macroscopic lung damage and demonstrated immature LBs on TEM, which was also observed on TEM from lung biopsy of participant 1. A study of *LAMP3* knockout mice revealed no evidence of neonatal respiratory distress or pulmonary abnormalities with normal lung morphology and cellular appearance of AT2 cells. However, when challenged with an induced allergic asthma model, these mice exhibited increased airway resistance and alterations in surfactant lipid composition, suggesting that LAMP3 plays a role in maintaining surfactant homeostasis under stress conditions.[22] Interestingly, analysis of the hydrophobic surfactant proteins in participant 1's BAL revealed no SP-B, an essential protein for normal biophysical surfactant activity. Because congenital absence of SP-B is not compatible with life and is typically associated with abundant pro-SP-C, which was not demonstrated here, our findings likely demonstrate a secondary deficiency or very low level of SP-B.[10,29] This may be due to ER retention and reduced alveolar delivery as a consequence of the *LAMP3* variant resulting in low protein level beyond the limit of detection of the WB technique used. Alternatively, this could be explained by enhanced alveolar removal by uptake into macrophages or intraalveolar proteolytic degradation. Prior studies using lung tissue from participant 5 similarly demonstrated reduced staining of SP-B.[27] Altogether, these studies provide evidence of a disruption to the pulmonary surfactant system due to variants in *LAMP3*.

The variable expressivity of *LAMP3* variants seen in this cohort resemble the diverse clinical course seen in patients with ILD caused by *ABCA3* missense or *SFTPC* variants.[9,12,46] Factors such as genotype, genetic variants at other loci, epigenetic variation, and environmental factors have been suggested to explain the variable clinical courses in patients with ABCA3 and SP-C dysfunction and may similarly account for the variability observed in our cohort.[9,47-50] Interestingly, although infants with biallelic *ABCA3* loss-of-function variants present with severe, progressive neonatal respiratory failure that is lethal in the first year of life without lung transplantation,[9,47,51] Participant 1 who is homozygous for a *LAMP* loss-of-function variant p.(Ile83PhefsTer47) also presented with severe neonatal respiratory failure but recovered after 10 days of mechanical ventilation. It is notable that the *LAMP3* knockout mice only demonstrated a respiratory phenotype under induced allergic conditions, which supports the potential role of environmental factors in symptom severity for *LAMP3*-associated conditions.[22] Infections or environmental exposures may also influence the development of airflow obstruction, suggestive of small airways disease, in addition to parenchymal lung disease with GGO and resultant lung fibrosis in some of the participants in this cohort. At this time, there is no definitive explanation for the variability in phenotypes seen in these families, and future studies exploring multifactorial contributions to the pulmonary phenotype of *LAMP3* variants are warranted.

Lung function studies from several participants in this cohort demonstrated mixed patterns with restriction and obstruction. Restrictive lung disease can be expected in ILD with the development of fibrosis. The presence of obstruction with air trapping in these participants is intriguing given that it is predominantly at the small airway level. Air trapping has been reported as a common and not unusual finding in ILD.[52] Additionally, increased airway resistance under allergic conditions was identified in the *LAMP3* knockout mouse model.[22] One possible explanation for the obstructive lung phenotype seen in this cohort is the development of small airway disease from loss of terminal bronchioles given that there is loss of AT2 cells due to LAMP3 deficiency. In chronic obstructive pulmonary disease, it is hypothesized that the loss of small airways is caused by collapse of the terminal bronchioles and alveolar ducts from a loss of tethering as the alveolar architecture becomes distorted from cell

variants ($n = 3$). $^{**}P < .01$ based on Student's t test. C and D. *LAMP3*-Gly288Arg and *LAMP3*-Gly388Arg variants inhibit cell growth. A549 cells were transfected with empty vector, *LAMP3*-WT, or *LAMP3*-Gly288Arg (C) or *LAMP3*-Gly388Arg (D) plasmids. Cells were counted 72 hours after replated with Countess Automated Cell Counter, $n = 8$. A549 $^{*}P < .05$, $^{**}p < 0.01$ based on Student's t test. E-H. A549 cells were transfected with empty vector, *LAMP3*-WT, or *LAMP3*-variants and cultured for 48 hours before imaging and flow cytometry with terminal deoxynucleotidyl transferase dUTP nick end labeling (TUNEL)/7-aminoactinomycin D (7-AAD) to quantify apoptotic cells. Bright-field microscopy at low (1) and high (2) magnification images with arrowheads showing examples of membrane-blebbing, which is characteristic for early apoptosis. I-P. Summary of flow cytometry data for TUNEL and 7-AAD-positive cells. Difference from positive and negative control cells is nonsignificant for *LAMP3*-Gly288Arg cells and significant for *LAMP3*-Gly388Arg cells by Student's t test ($^{*}P < .05$, $n = 4$).

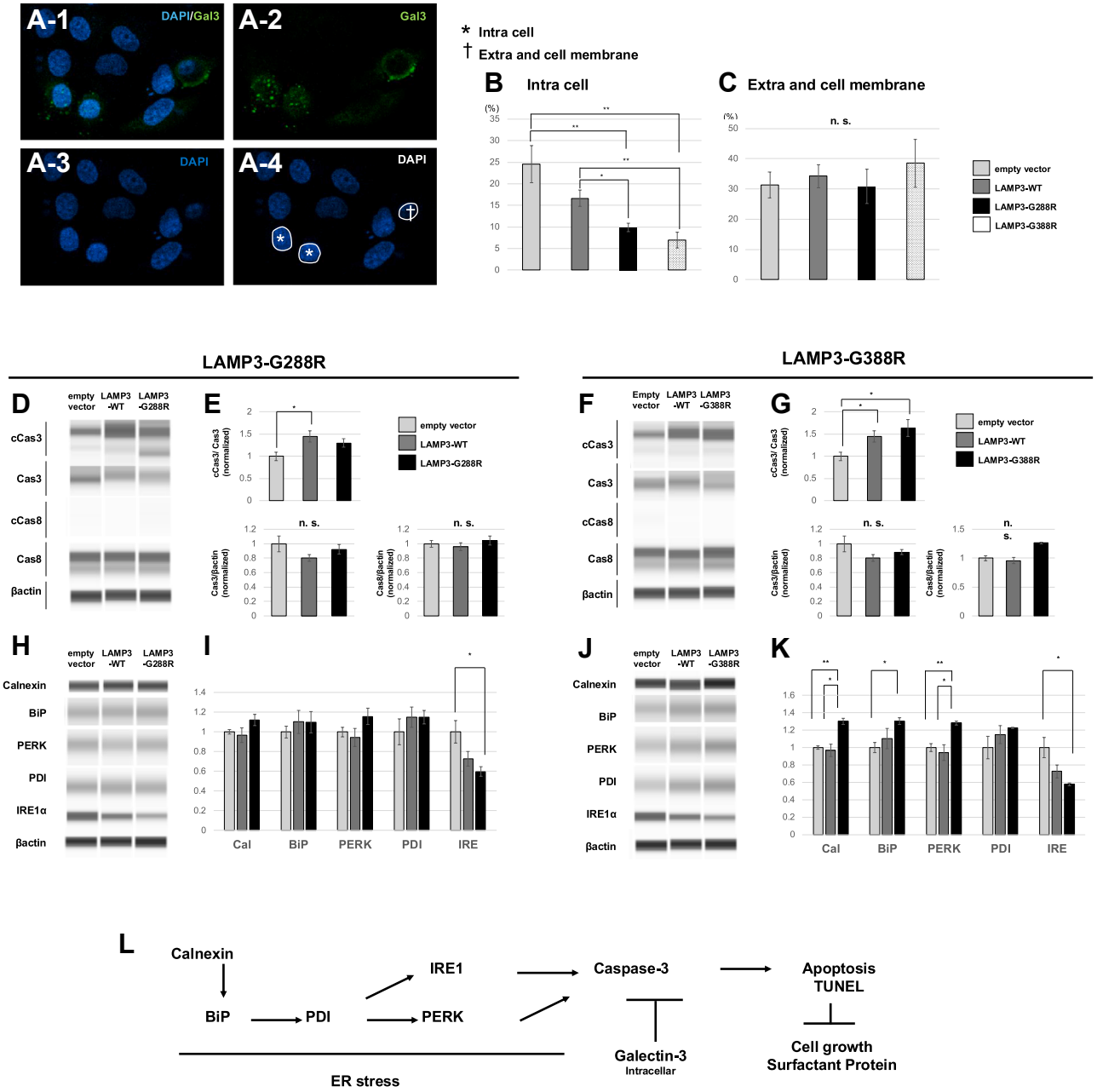

Figure 4 ***LAMP3*-Gly388Arg variant induces activation of caspase-3 and ER stress.** A. Representative immunofluorescence image shows staining for galectin-3 (green). *; Intracellular is defined as the LAMP3 positive cells in the intracellular space. †; Extracellular and cell membrane is defined the LAMP3 positive cells in the extracellular space and cell membrane. B. Bar chart shows the percentage of galectin-3 (Gal3) puncta-positive cells ($n = 8$). Percentage of cells expressing Gal3 intracellularly out of total cells between negative control (empty vector), positive control (*LAMP3*-WT), *LAMP3* variants (*LAMP3*-Gly288Arg or *LAMP3*-Gly388Arg). *$P < .05$, **$P < .01$, n.s.; nonsignificant. C. Percentage of cells expressing Gal3 extracellularly and within the cell membrane per total cell between empty vector, *LAMP3*-WT, *LAMP3*-Gly288Arg, and *LAMP3*-Gly388Arg. n.s.; nonsignificant. D. Caspase-3 (Cas3), cleaved-Caspase-3 (cCas3), Caspase-8 (Cas8), cleaved-Caspase-8 (cCas8), and βactin protein expression levels were measured by WB analysis in cells that express empty vector, *LAMP3*-WT, or *LAMP3*-Gly288Arg plasmids. E. WB analysis was performed to measure. cCas3/Cas3, Cas3/βactin and Cas8/βactin normalized by control. $n = 6$, $n = 6$, and $n = 3$. n.s.; nonsignificant based on Student's t test. F. WB analysis for cells that express empty vector, *LAMP3*-WT, or *LAMP3*-Gly388Arg plasmids. G. WB analysis was performed to measure cCas3/Cas3, Cas3/βactin and Cas8/βactin normalized by control. $n = 6$, $n = 6$, and $n = 3$. *$P < .05$. H. ER stress related protein expression levels were measured by WB analysis in cells that express empty vector, *LAMP3*-WT, or *LAMP3*-Gly288Arg plasmids. I. WB analysis was performed to measure and normalized by control, $n = 3$. n.s.; nonsignificant based on Student's t test. J. ER stress related protein expression levels were measured by WB analysis in cells that express empty vector, *LAMP3*-WT, or *LAMP3*-Gly388Arg plasmids. K. WB analysis was performed to measure and normalized by control, $n = 3$. *$P < .05$, **$P < .01$, n.s.; nonsignificant based on Student's t test. L. Schematic diagram of pathways from ER stress to the intrinsic apoptotic signaling pathway. These pathways converge at the activation of Cas3.

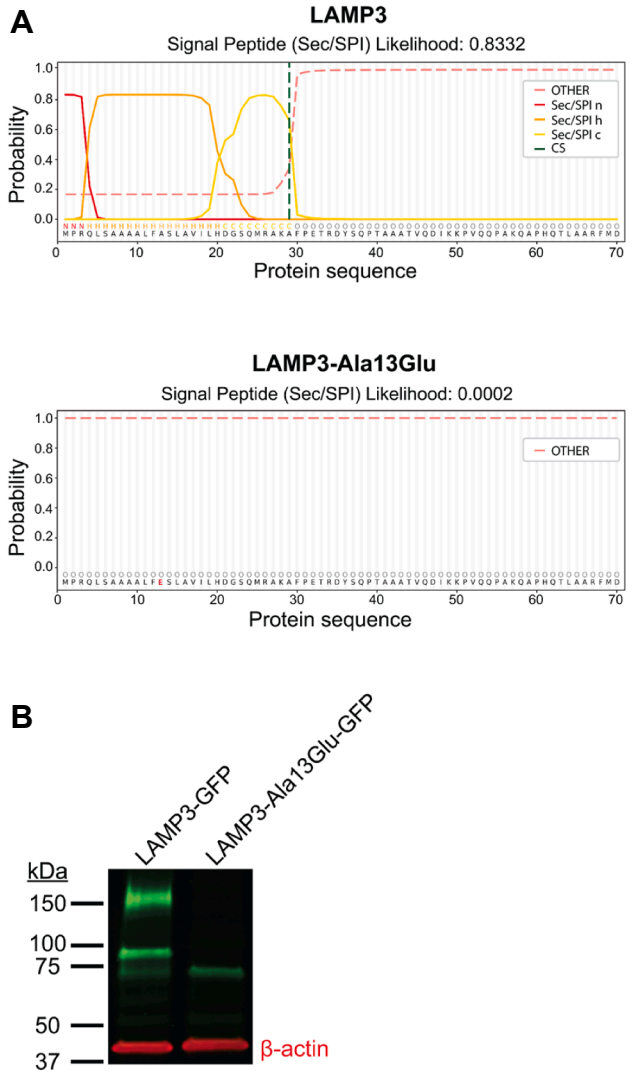

Figure 5 Compared with the wild-type protein, the *LAMP3*-Ala13Glu variant shows overall lower abundance and a reduced apparent molecular weight. A. Output from SignalP 6.0 showing the predicted Sec/SPI signal peptide on the N terminus of wild-type LAMP3 protein (top) and predicted loss of this signal in the LAMP3-Ala13Glu variant (bottom). In the figure key, Sec/SPI n = the N-terminal region of the signal peptide; Sec/SPI h = the central hydrophobic region; Sec/SPI c = the C-terminal region of the peptide; CS = the predicted signal peptide cleavage site; and OTHER indicates amino acid sequence outside of the signal peptide. B. Plasmids encoding GFP-tagged versions of the wild-type and Ala13Glu LAMP3 alleles were transiently transfected into A549 cells and cell lysates prepared at 24 hours after transfection. Lysates were separated by SDS-PAGE (20 µg total protein/lane) and WB using an antibody against the GFP tag.

death and inflammation.[53,54] An additional possibility to consider is that airway dysfunction is the result of abnormal resident DC function, given that DCs also highly express *LAMP3* and play a key role in innate immunity in the lung.[55] Further histologic evaluation of large airways in individuals with LAMP3 deficiency will be necessary to further elucidate the obstructive component of lung disease seen in the participants from this study.

Using a variety of in vitro biological endpoints, 2 of the *LAMP3* missense variants identified in this cohort p.(Gly288Arg) and p.(Gly388Arg) were found to cause abnormalities in the growth of lung A549 epithelial cells. Induced expression via transient transfection of both the *LAMP3*-Gly288Arg and *LAMP3*-Gly388Arg variants decreased cell growth. Interestingly, only 1 of the 2 variants, *LAMP3*-Gly388Arg, increased cell death via the intrinsic apoptosis pathway, involving increased ER stress and activation of Caspase-3, suggesting there may be differences in the pathobiology of the variants. The *LAMP3*-Ala13Glu variant causes reduced protein expression and abnormal protein glycosylation due to predicted loss of the signal peptide and abnormal cellular trafficking. Although these initial studies demonstrate in vitro abnormalities due to *LAMP3* variants, further detailed studies of these and other *LAMP3* variants are needed to elucidate the underlying pathophysiology of LAMP3 deficiency. Abnormalities in lysosomal membrane proteins are known to cause impaired autophagy and lysosomal dysfunction, which are crucial for maintaining intracellular homeostasis.[56-58] The expression of *LAMP3* in AT2 cells containing LBs suggests a specialized function in surfactant biogenesis. One limitation of our studies is that we used the A549 cell line, which although extensively used as a model for AT2 cells, does not model surfactant function well.[59,60] However, the in vitro studies presented here were primarily intended to evaluate effects on cell proliferation and viability. An additional limitation to consider is that A549 cells might not be optimal for the study of cellular function via transient transfection. Further studies are needed to evaluate the role of these *LAMP3* variants in the processing of SP-B and other surfactant proteins. Ideally, for these functional studies patient-derived induced AT2 cells (iAT2s) or CRISPR-edited lung cell lines with endogenous expression of patient-derived LAMP3 variants would be used for elucidating the role of *LAMP3* variants on LB and AT2 cell function, as has been performed for others genetic disorders of surfactant metabolism.[32,61,62]

Overall, this cohort serves as evidence of a disease-gene association for *LAMP3* in humans with variable expressivity. For patients with neonatal respiratory failure or ILD without a molecular diagnosis, evaluation for variants in *LAMP3* should be considered.

Data Availability

Individual level sequencing data for participant 1 is available through dbGAP accession number phs001232 (v5.p2). Additional data available from the authors upon request.

Acknowledgments

The authors thank the participants and their families. The authors thank Joan Wanqiong Qiao, PhD for her assistance in variant classification according to ACMG standards.

Funding

Research reported in this manuscript was supported in part by the NIH NINDS U01NS134358, NIDCR Z01-DE00695, and NHLBI R01HL149853. The content is solely the responsibility of the authors and does not necessarily represent the official views of the National Institutes of Health. Research was also supported by the Children's Discovery Institute at St Louis Children's Hospital/Washington University School of Medicine. The work of C. Milla was supported by the Ross Mosier Research Laboratories Gift Fund. The work of M. Griese was supported by German Research Foundation (Deutsche Forschungsgemeinschaft) 970/9-2 and the German Center for Lung Research (Deutsches Zentrum fur Lungenforschung). The work of P. McCray was supported by the Roy J. Carver Chair in Pulmonary Research and NHLBI R03 TR00481.

Author Contributions

Conceptualization: L.A.K., H.O.-M., C.M., O.B., J.A.Bernstein, J.A.C., M.H.; Data Curation: L.A.K., H.O.-M., C.M., O.B., J.A.Bernstein, J.A.C., M.H., P.D.B., M.H., J.R., D.H., F.S.C., J.A.W., D.J.W., D.B., N.N., C.L., T.D., M.G. J.A.Bartlett, P.B.M.Jr; Investigation: H.O.-M., J.A.Bartlett, P.B.M.Jr, M.G.; Visualization: L.A.K., H.O.-M., J.A.Bartlett, P.B.M.Jr., M.G.; Writing-original draft: L.A.K., H.O.-M.; Writing-reviewing and editing: L.A.K., H.O.-M., C.M., O.B., J.A.Bernstein, J.A.C., M.H., P.D.B., M.H., J.R., D.H., F.S.C., J.A.W., D.J.W., D.B., N.N., C.L., T.D., M.G., J.A.Bartlett, P.B.M.Jr; Supervision: C.M., O.B., J.A.Bernstein, J.A.C.

ORCID

Laura A. Keehan: http://orcid.org/0009-0005-3084-679X
Carlos Milla: http://orcid.org/0000-0001-5515-3053

Conflict of Interest

The authors declare no conflicts of interest.

Ethics Declaration

Written informed consent for publication was obtained from all participants. This study was reviewed under NIH IRB #15HG0130.

Additional Information

The online version of this article (https://doi.org/10.1016/j.gim.2026.102531) contains supplemental material, which is available to authorized users.

Members of the Undiagnosed Diseases Network

Alyssa A. Tran, Arjun Tarakad, Ashok Balasubramanyam, Brendan H. Lee, Carlos A. Bacino, Daryl A. Scott, Elaine Seto, Gary D. Clark, Hongzheng Dai, Hsiao-Tuan Chao, Ivan Chinn, James P. Orengo, Jennifer E. Posey, Jill A. Rosenfeld, Kim Worley, Lindsay C. Burrage, Lisa T. Emrick, Lorraine Potocki, Monika Weisz Hubshman, Richard A. Lewis, Ronit Marom, Seema R. Lalani, Shamika Ketkar, Tiphanie P. Vogel, William J. Craigen, Jared Sninsky, Lauren Blieden, Sandesh Nagamani, Hugo J. Bellen, Michael F. Wangler, Oguz Kanca, Shinya Yamamoto, Christine M. Eng, Patricia A. Ward, Pengfei Liu, Adeline Vanderver, Cara Skraban, Edward Behrens, Gonench Kilich, Kathleen Sullivan, Kelly Hassey, Ramakrishnan Rajagopalan, Rebecca Ganetzky, Vishnu Cuddapah, Anna Raper, Daniel J. Rader, Giorgio Sirugo, Vaidehi Jobanputra, Allyn McConkie-Rosell, Kelly Schoch, Mohamad Mikati, Nicole M. Walley, Rebecca C. Spillmann, Vandana Shashi, Alan H. Beggs, Calum A. MacRae, David A. Sweetser, Deepak A. Rao, Edwin K. Silverman, Elizabeth L. Fieg, Frances High, Gerard T. Berry, Ingrid A. Holm, J. Carl Pallais, Joan M. Stoler, Joseph Loscalzo, Lance H. Rodan, Laurel A. Cobban, Lauren C. Briere, Matthew Coggins, Melissa Walker, Richard L. Maas, Susan Korrick, Jessica Douglas, Cecilia Esteves, Emily Glanton, Isaac S. Kohane, Kimberly LeBlanc, Rachel Mahoney, Shamil R. Sunyaev, Shilpa N. Kobren, Brett H. Graham, Erin Conboy, Francesco Vetrini, Kayla M. Treat, Khurram Liaqat, Lili Mantcheva, Stephanie M. Ware, Breanna Mitchell, Brendan C. Lanpher, Devin Oglesbee, Eric Klee, Filippo Pinto e Vairo, Ian R. Lanza, Kahlen Darr, Lindsay Mulvihill, Lisa Schimmenti, Queenie Tan, Surendra Dasari, Abdul Elkadri, Brett Bordini, Donald Basel, James Verbsky, Julie McCarrier, Michael Muriello, Michael Zimmermann, Adriana Rebelo, Carson A. Smith, Deborah Barbouth, Guney Bademci, Joanna M. Gonzalez, Kumarie Latchman, LéShon Peart, Mustafa Tekin, Nicholas Borja, Stephan Zuchner, Stephanie Bivona, Willa Thorson, Herman Taylor, Rakale C. Quarells, Ayuko Iverson, Bruce

Gelb, Charlotte Cunningham-Rundles, Eric Gayle, Joanna Jen, Louise Bier, Mafalda Barbosa, Manisha Balwani, Mariya Shadrina, Rachel Evard, Saskia Shuman, Susan Shin, Andrea Gropman, Barbara N. Pusey Swerdzewski, Camilo Toro, Colleen E. Wahl, Donna Novacic, Ellen F. Macnamara, John J. Mulvihill, Maria T. Acosta, Precilla D'Souza, Valerie V. Maduro, Ben Afzali, Ben Solomon, Cynthia J. Tifft, David R. Adams, Elizabeth A. Burke, Francis Rossignol, Heidi Wood, Jiayu Fu, Joie Davis, Leoyklang Petcharet, Lynne A. Wolfe, Margaret Delgado, Marie Morimoto, Marla Sabaii, MayChristine V. Malicdan, Neil Hanchard, Orpa Jean-Marie, Wendy Introne, William A. Gahl, Yan Huang, Andrew Stergachis, Danny Miller, Elisabeth Rosenthal, Elizabeth Blue, Elsa Balton, Emily Shelkowitz, Eric Allenspach, Fuki M. Hisama, Gail P. Jarvik, Ghayda Mirzaa, Ian Glass, Kathleen A. Leppig, Katrina Dipple, Mark Wener, Martha Horike-Pyne, Michael Bamshad, Peter Byers, Runjun Kumar, Seth Perlman, Sirisak Chanprasert, Virginia Sybert, Wendy Raskind, Nitsuh K. Dargie, Chun-Hung Chan, Dr. Francisco Bustos Velasq, Isum Ward, Jason Schend, Jennifer Morgan, Megan Bell, Miranda Leitheiser, Mohamad Saifeddine, Paul Berger, Rachel Li, Taylor Beagle, Alexander Miller, Beatriz Anguiano, Beth A. Martin, Brianna Tucker, Chloe M. Reuter, Devon Bonner, Elijah Kravets, Hector Rodrigo Mendez, Holly K. Tabor, Jacinda B. Sampson, Jason Hom, Jennefer N. Kohler, Jennifer Schymick, John E. Gorzynski, Jonathan A. Bernstein, Kevin S. Smith, Laura Keehan, Laurens Wiel, Matthew T. Wheeler, Meghan C. Halley, Mia Levanto, Page C. Goddard, Paul G. Fisher, Rachel A. Ungar, Raquel L. Alvarez, Sara Emami, Shruti Marwaha, Stephen B. Montgomery, Suha Bachir, Tanner D. Jensen, Taylor Maurer, Terra R. Coakley, Euan A. Ashley, Ali Al-Beshri, Anna Hurst, Brandon M. Wilk, Bruce Korf, Elizabeth A. Worthey, Kaitlin Callaway, Martin Rodriguez, Tammi Skelton, Tarun KK Mamidi, Andrew B. Crouse, Jordan Whitlock, Mariko Nakano-Okuno, Matthew Might, William E. Byrd, Albert R. La Spada, Changrui Xiao, Elizabeth C. Chao, Eric Vilain, Jose Abdenur, Kirsten Blanco, Maija-Rikka Steenari, Rebekah Barrick, Richard Chang, Sanaz Attaripour, Suzanne Sandmeyer, Tahseen Mozaffar, Alden Huang, Andres Vargas, Bianca E. Russell, Brent L. Fogel, Esteban C. Dell'Angelica, George Carvalho, Julian A. Martínez-Agosto, Layal F. Abi Farraj, Manish J. Butte, Martin G. Martin, Naghmeh Dorrani, Neil H. Parker, Rosario I. Corona, Stanley F. Nelson, Yigit Karasozen, Aaron Quinlan, Alistair Ward, Ashley Andrews, Corrine K. Welt, Dave Viskochil, Erin E. Baldwin, John Carey, Justin Alvey, Laura Pace, Lorenzo Botto, Nicola Longo, Paolo Moretti, Rebecca Overbury, Russell Butterfield, Steven Boyden, Thomas J. Nicholas, Matt Velinder, Gabor Marth, Pinar Bayrak-Toydemir, Rong Mao, Monte Westerfield, Brian Corner, John A. Phillips III, Kimberly Ezell, Lynette Rives, Rizwan Hamid, Serena Neumann, Ashley McMinn, Joy D. Cogan, Thomas Cassini, Alex Paul, Dana Kiley, Daniel Wegner, Erin McRoy, Jennifer Wambach, Kathy Sisco, Patricia Dickson, F. Sessions Cole, Dustin Baldridge, Jimann Shin, Lilianna Solnica-Krezel, Stephen C. Pak, Timothy Schedl, Allen Bale, Carol Oladele, Caroline Hendry, Emily Wang, Hua Xu, Hui Zhang, Lauren Jeffries, María José Ortuño Romero, Mark Gerstein, Michele Spencer-Manzon, Monkol Lek, Nada Derar, Odelya Kaufman, Shrikant Mane, Teodoro Jerves Serrano, Vasilis Vasiliou, Winston Halstead, and Yong-Hui Jiang.

Affiliations

[1]Department of Pediatrics, Division of Medical Genetics, Stanford University School of Medicine, Stanford, CA; [2]Adeno-Associated Virus Biology Section, National Institute of Dental and Craniofacial Research, National Institutes of Health, Bethesda, MD; [3]Department of Oralfacial Disorders, Osaka University Graduate School of Dentistry, Suita, Osaka, Japan; [4]Pediatric Pulmonary Unit and Cystic fibrosis Center, Hadassah Medical Center and Faculty of Medicine, Hebrew University of Jerusalem, Israel; [5]Department of Genetics, Hadassah Medical Center and Faculty of Medicine, Hebrew University of Jerusalem, Israel; [6]Stead Family Department of Pediatrics, University of Iowa, IA; [7]Department of Pediatrics, Palestine Medical Complex, Ramallah, Palestine and Faculty of Medicine Al Quds University, East Jerusalem, Palestine; [8]Sorbonne University, Inserm UMR_S933 Laboratory of childhood genetic diseases, Armand Trousseau Hospital, Paris, France; [9]Department of Pediatric Pulmonology and Respi-Rare centre, Armand Trousseau Hospital, Assistance Publique Hôpitaux de Paris, France; [10]Biochemisches Institut, Christian-Albrechts-Universitaet; Kiel, Germany; [11]Section of Pediatric Pneumology; Dr. von Hauner Children's Hospital, LMU Munich, German Center for Lung research (DZL), Germany; [12]Edward Mallinckrodt Department of Pediatrics, Washington University School of Medicine and St Louis Children's Hospital, St Louis, MO; [13]Stanford Center for Undiagnosed Diseases, Stanford University, Stanford, CA; [14]Division of Cardiovascular Medicine, Stanford University School of Medicine, Stanford, CA; [15]Department of Pediatrics, Division of Pulmonary Medicine, Stanford University School of Medicine, Stanford, CA

References

1. Magnani JE, Donn SM. Persistent respiratory distress in the term neonate: genetic surfactant deficiency diseases. *Curr Pediatr Rev*. 2020;16(1):17-25. http://doi.org/10.2174/1573396315666190723112916
2. Nkadi PO, Merritt TA, Pillers D-AM. An overview of pulmonary surfactant in the neonate: genetics, metabolism, and the role of surfactant in health and disease. *Mol Genet Metab*. 2009;97(2):95-101. http://doi.org/10.1016/j.ymgme.2009.01.015
3. Veldhuizen R, Possmayer F. Phospholipid metabolism in lung surfactant. *Subcell Biochem*. 2004;37:359-388. http://doi.org/10.1007/978-1-4757-5806-1_11
4. Nogee LM. Interstitial lung disease in newborns. *Semin Fetal Neonatal Med*. 2017;22(4):227-233. http://doi.org/10.1016/j.siny.2017.03.003

5. Singh J, Jaffe A, Schultz A, Selvadurai H. Surfactant protein disorders in childhood interstitial lung disease. *Eur J Pediatr*. 2021;180(9):2711-2721. http://doi.org/10.1007/s00431-021-04066-3
6. Floros J, Tsotakos N. Differential regulation of human surfactant protein A genes, SFTPA1 and SFTPA2, and their corresponding variants. *Front Immunol*. 2021;12:766719. http://doi.org/10.3389/fimmu.2021.766719
7. Hamvas A. Inherited surfactant protein-B deficiency and surfactant protein-C associated disease: clinical features and evaluation. *Semin Perinatol*. 2006;30(6):316-326. http://doi.org/10.1053/j.semperi.2005.11.002
8. Cooney AL, Wambach JA, Sinn PL, McCray PB. Gene therapy potential for genetic disorders of surfactant dysfunction. *Front Genome Ed*. 2021;3:785829. http://doi.org/10.3389/fgeed.2021.785829
9. Wambach JA, Casey AM, Fishman MP, et al. Genotype-phenotype correlations for infants and children with ABCA3 deficiency. *Am J Respir Crit Care Med*. 2014;189(12):1538-1543. http://doi.org/10.1164/rccm.201402-0342OC
10. Nogee LM, Wert SE, Proffit SA, Hull WM, Whitsett JA. Allelic heterogeneity in hereditary surfactant protein B (SP-B) deficiency. *Am J Respir Crit Care Med*. 2000;161(3 Pt 1):973-981. http://doi.org/10.1164/ajrccm.161.3.9903153
11. Eldridge WB, Zhang Q, Faro A, et al. Outcomes of lung transplantation for infants and children with genetic disorders of surfactant metabolism. *J Pediatr*. 2017;184:157-164.e2. http://doi.org/10.1016/j.jpeds.2017.01.017
12. Si X, Steffes LC, Schymick JC, Hazard FK, Tracy MC, Cornfield DN. Three infants with pathogenic variants in the ABCA3 gene: presentation, treatment, and clinical course. *J Pediatr*. 2021;231:278-283.e2. http://doi.org/10.1016/j.jpeds.2020.12.055
13. Brudon A, Legendre M, Mageau A, et al. High risk of lung cancer in surfactant-related gene variant carriers. *Eur Respir J*. 2024;63(5):2301809. http://doi.org/10.1183/13993003.01809-2023
14. Sitaraman S, Alysandratos K-D, Wambach JA, Limberis MP. Gene therapeutics for surfactant dysfunction disorders: targeting the alveolar Type 2 epithelial cell. *Hum Gene Ther*. 2022;33(19-20):1011-1022. http://doi.org/10.1089/hum.2022.130
15. Hamvas A, Deterding RR, Wert SE, et al. Heterogeneous pulmonary phenotypes associated with mutations in the thyroid transcription factor gene NKX2-1. *Chest*. 2013;144(3):794-804. http://doi.org/10.1378/chest.12-2502
16. Nogee LM, Dunbar AE, Wert SE, Askin F, Hamvas A, Whitsett JA. A mutation in the surfactant protein C gene associated with familial interstitial lung disease. *N Engl J Med*. 2001;344(8):573-579. http://doi.org/10.1056/NEJM200102223440805
17. Soreze Y, Nathan N, Jegard J, et al. Acinar dysplasia in a full-term newborn with a NKX2.1 variant. *Neonatology*. 2024;121(1):133-136. http://doi.org/10.1159/000534076
18. GTEx Consortium. The Genotype-Tissue Expression (GTEx) project. *Nat Genet*. 2013;45(6):580-585. http://doi.org/10.1038/ng.2653
19. Salaun B, de Saint-Vis B, Pacheco N, et al. CD208/dendritic cell-lysosomal associated membrane protein is a marker of normal and transformed type II pneumocytes. *Am J Pathol*. 2004;164(3):861-871. http://doi.org/10.1016/S0002-9440(10)63174-4
20. Weichert N, Kaltenborn E, Hector A, et al. Some ABCA3 mutations elevate ER stress and initiate apoptosis of lung epithelial cells. *Respir Res*. 2011;12(1):4. http://doi.org/10.1186/1465-9921-12-4
21. Nakamura H, Tanaka T, Zheng C, et al. Correction of LAMP3-associated salivary gland hypofunction by aquaporin gene therapy. *Sci Rep*. 2022;12(1):18570. http://doi.org/10.1038/s41598-022-21374-2
22. Lunding LP, Krause D, Stichtenoth G, et al. LAMP3 deficiency affects surfactant homeostasis in mice. *PLoS Genet*. 2021;17(6):e1009619. http://doi.org/10.1371/journal.pgen.1009619
23. Akasaki K, Nakamura N, Tsukui N, et al. Human dendritic cell lysosome-associated membrane protein expressed in lung type II pneumocytes. *Arch Biochem Biophys*. 2004;425(2):147-157. http://doi.org/10.1016/j.abb.2004.02.042
24. Albrecht S, Usmani SM, Dietl P, Wittekindt OH. Plasma membrane trafficking in alveolar type II cells. *Cell Physiol Biochem*. 2010;25(1):81-90. http://doi.org/10.1159/000272053
25. Dillard KJ, Ochs M, Niskanen JE, et al. Recessive missense LAMP3 variant associated with defect in lamellar body biogenesis and fatal neonatal interstitial lung disease in dogs. *PLoS Genet*. 2020;16(3):e1008651. http://doi.org/10.1371/journal.pgen.1008651
26. Rips J, Halstuk O, Fuchs A, et al. Unbiased phenotype and genotype matching maximizes gene discovery and diagnostic yield. *Genet Med*. 2024;26(4):101068. http://doi.org/10.1016/j.gim.2024.101068
27. Louvrier C, Desroziers T, Soreze Y, et al. Bi-allelic LAMP3 variants in childhood interstitial lung disease: a surfactant-related disease. *EBioMedicine*. 2025;113:105626. http://doi.org/10.1016/j.ebiom.2025.105626
28. Sobreira N, Schiettecatte F, Valle D, Hamosh A. GeneMatcher: a matching tool for connecting investigators with an interest in the same gene. *Hum Mutat*. 2015;36(10):928-930. http://doi.org/10.1002/humu.22844
29. Griese M, Lorenz E, Hengst M, et al. Surfactant proteins in pediatric interstitial lung disease. *Pediatr Res*. 2016;79(1-1):34-41. http://doi.org/10.1038/pr.2015.173
30. Tafel O, Latzin P, Paul K, Winter T, Woischnik M, Griese M. Surfactant proteins SP-B and SP-C and their precursors in bronchoalveolar lavages from children with acute and chronic inflammatory airway disease. *BMC Pulm Med*. 2008;8:6. http://doi.org/10.1186/1471-2466-8-6
31. Tanaka T, Warner BM, Michael DG, et al. LAMP3 inhibits autophagy and contributes to cell death by lysosomal membrane permeabilization. *Autophagy*. 2021;18(7):1629-1647. http://doi.org/10.1080/15548627.2021.1995150
32. Sun YL, Hennessey EE, Heins H, et al. Human pluripotent stem cell modeling of alveolar type 2 cell dysfunction caused by ABCA3 mutations. *J Clin Invest*. 2024;134(2):e164274. http://doi.org/10.1172/JCI164274
33. Chen S, Francioli LC, Goodrich JK, et al. A genomic mutational constraint map using variation in 76,156 human genomes. *Nature*. 2024;625(7993):92-100. http://doi.org/10.1038/s41586-023-06045-0
34. Rentzsch P, Witten D, Cooper GM, Shendure J, Kircher M. CADD: predicting the deleteriousness of variants throughout the human genome. *Nucleic Acids Res*. 2019;47(D1):D886-D894. http://doi.org/10.1093/nar/gky1016
35. de Sainte Agathe J-M, Filser M, Isidor B, et al. SpliceAI-visual: a free online tool to improve SpliceAI splicing variant interpretation. *Hum Genomics*. 2023;17(1):7. http://doi.org/10.1186/s40246-023-00451-1
36. Richards S, Aziz N, Bale S, et al. Standards and guidelines for the interpretation of sequence variants: a joint consensus recommendation of the American College of Medical Genetics and Genomics and the Association for Molecular Pathology. *Genet Med*. 2015;17(5):405-424. http://doi.org/10.1038/gim.2015.30
37. Strande NT, Riggs ER, Buchanan AH, et al. Evaluating the clinical validity of gene-disease associations: an evidence-based framework developed by the clinical genome resource. *Am J Hum Genet*. 2017;100(6):895-906. http://doi.org/10.1016/j.ajhg.2017.04.015
38. Orrenius S. Mitochondrial regulation of apoptotic cell death. *Toxicol Lett*. 2004;149(1-3):19-23. http://doi.org/10.1016/j.toxlet.2003.12.017
39. Gilson RC, Gunasinghe SD, Johannes L, Gaus K. Galectin-3 modulation of T-cell activation: mechanisms of membrane remodelling. *Prog Lipid Res*. 2019;76:101010. http://doi.org/10.1016/j.plipres.2019.101010
40. Tabas I, Ron D. Integrating the mechanisms of apoptosis induced by endoplasmic reticulum stress. *Nat Cell Biol*. 2011;13(3):184-190. http://doi.org/10.1038/ncb0311-184
41. Teufel F, Almagro Armenteros JJ, Johansen AR, et al. SignalP 6.0 predicts all five types of signal peptides using protein language models. *Nat Biotechnol*. 2022;40(7):1023-1025. http://doi.org/10.1038/s41587-021-01156-3
42. de Saint-Vis B, Vincent J, Vandenabeele S, et al. A novel lysosome-associated membrane glycoprotein, DC-LAMP, induced upon DC maturation, is transiently expressed in MHC Class II compartment.

Immunity. 1998;9(3):325-336. http://doi.org/10.1016/S1074-7613(00)80615-9
43. Engelbrecht S, Kaltenborn E, Griese M, Kern S. The surfactant lipid transporter ABCA3 is N-terminally cleaved inside LAMP3-positive vesicles. *FEBS Lett*. 2010;584(20):4306-4312. http://doi.org/10.1016/j.febslet.2010.09.026
44. Alessandrini F, Pezzè L, Ciribilli Y. LAMPs: shedding light on cancer biology. *Semin Oncol*. 2017;44(4):239-253. http://doi.org/10.1053/j.seminoncol.2017.10.013
45. Cunningham AC, Milne DS, Wilkes J, Dark JH, Tetley TD, Kirby JA. Constitutive expression of mhc and adhesion molecules by alveolar epithelial cells (type II pneumocytes) isolated from human lung and comparison with immunocytochemical findings. *J Cell Sci*. 1994;107(2):443-449. http://doi.org/10.1242/jcs.107.2.443
46. Hallik M, Annilo T, Ilmoja M-L. Different course of lung disease in two siblings with novel ABCA3 mutations. *Eur J Pediatr*. 2014;173(12):1553-1556. http://doi.org/10.1007/s00431-013-2087-3
47. Kröner C, Wittmann T, Reu S, et al. Lung disease caused by ABCA3 mutations. *Thorax*. 2017;72(3):213-220. http://doi.org/10.1136/thoraxjnl-2016-208649
48. Beers MF, Mulugeta S. The biology of the ABCA3 lipid transporter in lung health and disease. *Cell Tissue Res*. 2017;367(3):481-493. http://doi.org/10.1007/s00441-016-2554-z
49. Xu KK, Wegner DJ, Geurts LC, et al. Biologic characterization of ABCA3 variants in lung tissue from infants and children with ABCA3 deficiency. *Pediatr Pulmonol*. 2022;57(5):1325-1330. http://doi.org/10.1002/ppul.25862
50. Tomer Y, Wambach J, Knudsen L, et al. The common ABCA3E292V variant disrupts AT2 cell quality control and increases susceptibility to lung injury and aberrant remodeling. *Am J Physiol Lung Cell Mol Physiol*. 2021;321(2):L291-L307. http://doi.org/10.1152/ajplung.00400.2020
51. Li Y, Seidl E, Knoflach K, et al. ABCA3-related interstitial lung disease beyond infancy. *Thorax*. 2023;78(6):587-595. http://doi.org/10.1136/thorax-2022-219434
52. Hochhegger B, Sanches FD, Altmayer SPL, et al. Air trapping in usual interstitial pneumonia pattern at CT: prevalence and prognosis. *Sci Rep*. 2018;8(1):17267. http://doi.org/10.1038/s41598-018-35387-3
53. Booth S, Hsieh A, Mostaco-Guidolin L, et al. A single-cell atlas of small airway disease in chronic obstructive pulmonary disease: a cross-sectional study. *Am J Respir Crit Care Med*. 2023;208(4):472-486. http://doi.org/10.1164/rccm.202303-0534OC
54. Mitzner W. Emphysema—a disease of small airways or lung parenchyma? *N Engl J Med*. 2011;365(17):1637-1639. http://doi.org/10.1056/NEJMe1110635
55. Lambrecht BN, Prins JB, Hoogsteden HC. Lung dendritic cells and host immunity to infection. *Eur Respir J*. 2001;18(4):692-704. http://doi.org/10.1183/09031936.01.18040692
56. Ballabio A, Gieselmann V. Lysosomal disorders: from storage to cellular damage. *Biochim Biophys Acta*. 2009;1793(4):684-696. http://doi.org/10.1016/j.bbamcr.2008.12.001
57. Walkley SU. Pathogenic mechanisms in lysosomal disease: a reappraisal of the role of the lysosome. *Acta Paediatr*. 2007;96(455):26-32. http://doi.org/10.1111/j.1651-2227.2007.00202.x
58. Appelqvist H, Wäster P, Kågedal K, Öllinger K. The lysosome: from waste bag to potential therapeutic target. *J Mol Cell Biol*. 2013;5(4):214-226. http://doi.org/10.1093/jmcb/mjt022
59. Cooper JR, Abdullatif MB, Burnett EC, et al. Long term culture of the A549 cancer cell line promotes multilamellar body formation and differentiation towards an alveolar Type II pneumocyte phenotype. *PLoS One*. 2016;11(10):e0164438. http://doi.org/10.1371/journal.pone.0164438
60. Swain RJ, Kemp SJ, Goldstraw P, Tetley TD, Stevens MM. Assessment of cell line models of primary human cells by Raman spectral phenotyping. *Biophys J*. 2010;98(8):1703-1711. http://doi.org/10.1016/j.bpj.2009.12.4289
61. Jacob A, Morley M, Hawkins F, et al. Differentiation of human pluripotent stem cells into functional lung alveolar epithelial cells. *Cell Stem Cell*. 2017;21(4):472-488.e10. http://doi.org/10.1016/j.stem.2017.08.014
62. Alysandratos K-D, Russo SJ, Petcherski A, et al. Patient-specific iPSCs carrying an SFTPC mutation reveal the intrinsic alveolar epithelial dysfunction at the inception of interstitial lung disease. *Cell Rep*. 2021;36(9):109636. http://doi.org/10.1016/j.celrep.2021.109636